

Effect of the Crystal Packing and LIESST Effect of a Two-Dimensional Iron(II) Spin-Crossover Complex: $[Fe^{II}(HL^{H,Me})_2](CF_3SO_3)_2$ ($HL^{H,Me}$: 8-(Imidazol-4-ylmethylideneamino)-2-methylquinoline)

Hiroaki Hagiwara,* Osamu Sakaguchi, Koshiro Nishi, Shingo Hashimoto, and Naohide Matsumoto*

Department of Chemistry, Graduate School of Science and Technology, Kumamoto University, 2-39-1 Kurokami, Kumamoto 860-8555

Received May 12, 2011; E-mail: 107d9006@st.kumamoto-u.ac.jp, naohide@aster.sci.kumamoto-u.ac.jp

A 2D iron(II) spin-crossover (SCO) complex, $[Fe^{II}(HL^{H,Me})_2](CF_3SO_3)_2$, was synthesized, where $HL^{H,Me}$: 8-(imidazol-4-ylmethylideneamino)-2-methylquinoline, and its structures and magnetic properties were investigated. The complex $[Fe^{II}(HL^{H,Me})_2](CF_3SO_3)_2$ has no crystal solvent and has structure isomorphous to the complex $[Fe^{II}(HL^{H,Me})_2](ClO_4)_2 \cdot 1.5MeCN$, and shows a gradual and reversible one-step SCO between the HS ($S = 2$) and LS ($S = 0$) states at $T_{1/2} = 215$ K without hysteresis. The $T_{1/2}$ value is higher than that of corresponding desolvated ClO_4^- compound, $[Fe^{II}(HL^{H,Me})_2](ClO_4)_2$, about 35 K, although the spin transition is more gradual than that of ClO_4^- compound and the hysteresis is absent, which is observed in ClO_4^- compound. The crystal structures were determined at 296 (HS state) and 100 K (LS state), where the crystal system and space group showed no change between these temperatures. The structures at both temperatures have the same 2D layered structure, which is constructed of both the bifurcated NH···O^- hydrogen bonds between two $CF_3SO_3^-$ ions and two neighboring imidazole NH groups of the $[Fe^{II}(HL^{H,Me})_2]^{2+}$ cations and the π–π interactions between the two quinolyl rings of the two adjacent cations. This network structure is the same as that of ClO_4^- compound. 600 nm light irradiation at 10 K induced the LIESST effect.

Spin crossover (SCO) is a representative example of molecular bistability, in which the high-spin (HS) and low-spin (LS) states are interconvertible by physical perturbations such as temperature, pressure, and light.[1] Because it has potential applications in switching and sensing devices,[2] SCO complexes have attracted much attention in the last decade.[1a] Among the d^4–d^7 electronic configurations, iron(II) SCO complexes with d^6 electronic configuration have been most extensively studied.[1] While SCO is essentially described as a phenomenon of a single molecule, interesting SCO behaviors observed in the solid state, such as steep, multistep SCO, and hysteresis, have been ascribed to a cooperative effect between the SCO sites.[1] From the synthetic viewpoint to achieve a cooperative effect, polymeric SCO complexes with bridging ligands[3] and mononuclear SCO complexes exhibiting intermolecular hydrogen bonding[4] or π–π stacking[5] have been synthesized and among them interesting SCO behaviors were discovered. From the theoretical side, Ising-like models have been used in order to take into account the cooperativity in the SCO transition[6] and the origin of the cooperative nature has been investigated by considering elastic interactions among molecules.[7] However, the parameters of the theoretical model calculations are not well correlated with the real molecular structure of SCO complex. In practice, the SCO properties are influenced complicatedly by subfactors such as the counter anion and crystal solvent. Therefore, it seems to be difficult to establish the correlation between the theoretical parameters and the structural parameters. In order to approach this problem, a series of SCO complexes exhibiting the same network structure and showing different SCO properties is helpful to understand the spin transition behavior from synthetic and theoretical viewpoints.

Recently, we[8,9] and others[10] have investigated iron complexes with tripodal ligands containing three imidazole groups. Of these, we have reported a series of SCO complexes exhibiting the same network structure and different SCO properties.[9] A series of complexes $[Fe^{II}H_3L^{Me}]X \cdot Y$ ($X^- = Cl^-$, $Y^- = PF_6^-$, AsF_6^-, SbF_6^-, $CF_3SO_3^-$, and $X \cdot Y = Br \cdot CF_3SO_3$), where H_3L^{Me} is a hexadentate N_6 tripodal ligand of the neutral form, tris[2-(2-methylimidazol-4-ylmethylideneamino)ethyl]-amine, were isomorphous to each other and showed a variety of SCO behaviors, (1) a one-step SCO of HS $\leftrightarrows$ (HS + LS)/2, (2) a two-step SCO of HS $\leftrightarrows$ (HS + LS)/2 $\leftrightarrows$ LS, (3) a gradual one-step SCO of HS $\leftrightarrows$ LS, and (4) a steep one-step SCO of HS $\leftrightarrows$ LS with hysteresis. They had the common crystal structure consisting of a 2D extended network structure, which is constructed by NH···X^- hydrogen bonds between halogen ion X^- and the imidazole NH groups of three neighboring cations $[Fe^{II}H_3L^{Me}]^{2+}$ and the anion Y^- exists just as an isolated counter anion and occupies the space among the 2D sheets. On the basis of this study, (1) the effect of the size and shape of counter anion Y^- that is not involved in the network structure and just occupies the interlayer of the 2D layer and (2) the influence of the connecting halogen ion involved in the framework of the network structure on their SCO properties were revealed.

We have also reported another type of 2D iron(II) SCO complex, $[Fe^{II}(HL^{H,Me})_2](ClO_4)_2 \cdot 1.5MeCN$, where $HL^{H,Me}$ is tridentate N_3 ligand, 8-(imidazol-4-ylmethylideneamino)-2-methylquinoline (Chart 1).[11] This complex showed a desolva-

Published on the web August 23, 2011; doi:10.1246/bcsj.20110136

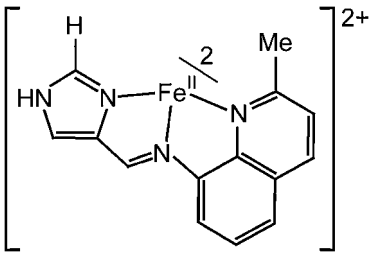

Chart 1. Schematic drawing of $[Fe^{II}(HL^{H,Me})_2]^{2+}$.

tion induced steep one-step spin transition with a thermal hysteresis of 11 K and had the 2D layered structure, which is constructed of both the bifurcated NH···O^- hydrogen bonds between two ClO_4^- ions and two neighboring imidazole NH groups of the $[Fe^{II}(HL^{H,Me})_2]^{2+}$ cations and the π–π interactions between the two quinolyl rings of the two adjacent cations. In this system, steep SCO with hysteresis was mainly brought by the extended 2D network, which has structural flexibility due to the desolvation of MeCN, exists only in an intralayer cavity of the 2D structure. This suggests that not only a network structure that makes possible a spin transition over all SCO sites, but also structural fitness or flexibility giving large structural change in the crystal lattice have an important role in acquiring cooperative SCO in the present system.

In this work, an analogous 2D SCO iron(II) complex, $[Fe^{II}(HL^{H,Me})_2](CF_3SO_3)_2$, was prepared to investigate in more detail the effect of crystal packing. It was found that the present complex had no crystal solvent and showed a gradual and reversible one-step SCO without hysteresis, although it had structure isomorphous to the corresponding ClO_4^- complex, $[Fe^{II}(HL^{H,Me})_2](ClO_4)_2 \cdot 1.5MeCN$. This is mainly due to the tight crystal packing of the intralayer spaces of the 2D network. We report here the synthesis, structure, and the SCO properties with LIESST (light-induced excited spin state trapping) effect.

Results and Discussion

Synthesis. It should be noted that $[Fe^{II}(HL^{H,Me})_2](CF_3SO_3)_2$ was synthesized in air. The tridentate ligand was prepared by the 1:1 condensation reaction of 4-formylimidazole and 8-amino-2-methylquinoline in methanol, and the resulting ligand solution was used for the synthesis of complex. The complex was prepared by mixing the methanol solution of the tridentate ligand and $Fe^{II}(CF_3SO_3)_2$ in 2:1 molar ratios, where black block crystals precipitated and were collected by suction filtration. The formula of $[Fe^{II}(HL^{H,Me})_2](CF_3SO_3)_2$ was confirmed by elemental analysis. The infrared (IR) spectra showed a characteristic band at 1610 cm^{-1}, assigned to the C=N stretching vibration of the Schiff-base ligand. The complex showed thermochromism from black at ambient temperature to dark-green at liquid nitrogen temperature.

Magnetic Properties of $[Fe^{II}(HL^{H,Me})_2](CF_3SO_3)_2$. The magnetic susceptibilities of the polycrystalline samples were measured in the temperature range of 5–350 K at a sweep rate of 1 K min^{-1} under an applied magnetic field of 0.5 T. The sample was quickly cooled to 5 K from room temperature and the magnetic susceptibility was measured while raising the temperature from 5 to 350 K. Subsequently, the magnetic susceptibility was measured while lowering the temperature

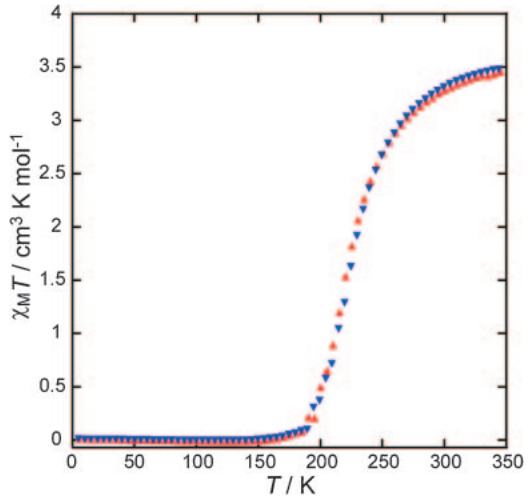

Figure 1. Magnetic behavior of $[Fe^{II}(HL^{H,Me})_2](CF_3SO_3)_2$ in the form of $\chi_M T$ vs. T plots. The sample was quickly cooled from room temperature to 5 K and $\chi_M T$ values were first measured in the course of warming from 5 to 350 K at a sweep rate of 1 K min^{-1} (▲). $\chi_M T$ values were then measured in the course of cooling from 350 to 5 K (▼).

from 350 to 5 K. The $\chi_M T$ vs. T plots for the ground sample are shown in Figure 1, demonstrating a complete one-step SCO between HS ($S = 2$) and LS ($S = 0$) states, where χ_M is the molar magnetic susceptibility and T is the absolute temperature. The magnetic behaviors are very similar in the heating and cooling indicating the absence of a frozen-in effect and thermal hysteresis. In the temperature region higher than 295 K, the constant $\chi_M T$ value of ca. 3.4 cm^3 K mol^{-1} is compatible with the expected value for HS Fe^{II} ($S = 2$) complexes. In the temperature region lower than 185 K, a plateau value of ca. 0.0 cm^3 K mol^{-1} is compatible with the expected value for LS Fe^{II} ($S = 0$) complexes. In the region of the spin transition temperature, the $\chi_M T$ value changes rather gradually from ca. 0.0 cm^3 K mol^{-1} at 185 K to ca. 3.4 cm^3 K mol^{-1} at 295 K between the HS and LS values without hysteresis. The SCO transition temperature $T_{1/2}$ can be evaluated to be $T_{1/2} = 215$ K by the calculation of the derivative $d(\chi_M T)/dT$.

Crystal Structure of $[Fe^{II}(HL^{H,Me})_2](CF_3SO_3)_2$. The X-ray diffraction data were collected at 296 (HS state) and 100 K (LS state). The crystallographic data at 296 and 100 K are given in Table 1 with those of the corresponding ClO_4^- compound, $[Fe^{II}(HL^{H,Me})_2](ClO_4)_2 \cdot 1.5MeCN$.[11] The structure consists of a cation $[Fe^{II}(HL^{H,Me})_2]^{2+}$ and two anions of $CF_3SO_3^-$. Table 1 demonstrates that the structures at both temperatures and those of the corresponding ClO_4^- compound are isomorphous to each other.[11] The dimensions of the unit cell parameters are similar to each other and the cell volume is reduced by 3.0% associated with the spin transition. The crystal structures at the two temperatures have the same 2D layered structure and are the same as that of corresponding ClO_4^- compound.

At 296 K: The molecular structure with the atom numbering scheme at 296 K is shown in Figure 2, and selected bond lengths and angles are given in Table 2. The Fe^{II} ion assumes an octahedral coordination environment and is made

Table 1. X-ray Crystallographic Data for $[Fe^{II}(HL^{H,Me})_2](CF_3SO_3)_2$ at 296 and 100 K and Corresponding ClO_4^- Complex, $[Fe^{II}(HL^{H,Me})_2](ClO_4)_2 \cdot 1.5MeCN$, at 296 and 150 K[11]

	$[Fe^{II}(HL^{H,Me})_2](CF_3SO_3)_2$		$[Fe^{II}(HL^{H,Me})_2](ClO_4)_2 \cdot 1.5MeCN$[11]	
	296 K	100 K	296 K	150 K
Formula	$C_{30}H_{24}N_8FeF_6S_2O_6$	$C_{30}H_{24}N_8FeF_6S_2O_6$	$C_{31}H_{28.5}N_{9.5}FeCl_2O_8$	$C_{31}H_{28.5}N_{9.5}FeCl_2O_8$
Formula weight	826.53	826.53	788.88	788.88
Crystal system	Monoclinic	Monoclinic	Monoclinic	Monoclinic
Space group	$C2/c$	$C2/c$	$C2/c$	$C2/c$
a/Å	18.570(8)	18.604(7)	19.733(8)	19.563(7)
b/Å	13.621(5)	13.345(5)	12.901(5)	12.713(5)
c/Å	16.556(7)	16.260(5)	17.025(6)	16.837(8)
β/degree	117.767(14)	117.116(14)	121.261(15)	121.099(15)
V/Å^3	3705(3)	3593(2)	3704.9(24)	3585.6(26)
Z	4	4	4	4
T/K	296	100	296	150
d_{calcd}/g cm^{-3}	1.481	1.528	1.414	1.461
μ/cm^{-1}	6.013	6.200	6.111	6.315
R[a], R_w[b]	0.0598, 0.1290	0.0440, 0.1410	0.0759, 0.1677	0.0762, 0.1749

a) $R = \Sigma||F_o| - |F_c||/\Sigma|F_o|$. b) $R_w = [\Sigma w(|F_o^2| - |F_c^2|)^2/\Sigma w|F_o^2|^2]^{1/2}$.

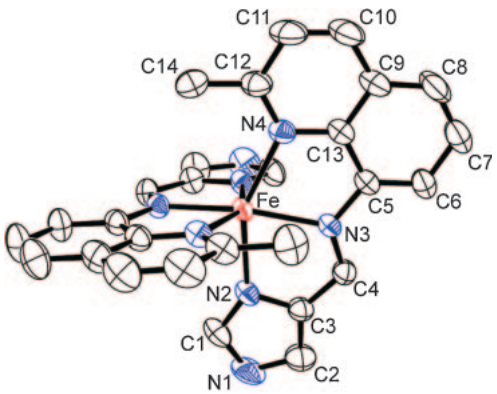

Figure 2. Molecular structure of $[Fe^{II}(HL^{H,Me})_2](CF_3SO_3)_2$ at 296 K with the atom numbering scheme, where the thermal ellipsoids are drawn with a 50% probability level. $CF_3SO_3^-$ ions and H atoms are omitted for clarity.

up of the six N donor atoms of two tridentate $HL^{H,Me}$ ligands. The iron atom lies on a 2-fold rotation axis, and this defines the crystallographically unique unit as a half of the cation $[Fe^{II}(HL^{H,Me})_2]^{2+}$. At 296 K, the Fe–N bond lengths are in the range of 2.1220(19)–2.183(2) Å, and the average Fe–N bond length is 2.160 Å, which are slightly shorter than the values expected for the HS Fe^{II} complex with similar N_6 donor atoms and longer than those for LS complex. The distances of Fe–$N_{imidazole}$, Fe–N_{imine}, and Fe–$N_{quinoline}$ are 2.174(3), 2.1220(19), and 2.183(2) Å, respectively. It is noteworthy that the coordination bond distance of Fe–N_{imine} is shorter than those of Fe–$N_{imidazole}$ and Fe–$N_{quinoline}$.

Intermolecular interactions and the extended network structure at 296 K are shown in Figure 3 and Figures 4a and 4b, respectively. As shown in Figures 3 and 4a, the $CF_3SO_3^-$ ions play the role of connector through bifurcated hydrogen bonds between O^- and the imidazole NH groups of two neighboring cations $[Fe^{II}(HL^{H,Me})_2]^{2+}$. Two $CF_3SO_3^-$ ions are hydrogen-bonded to the imidazole NH groups of two neighboring cations $[Fe^{II}(HL^{H,Me})_2]^{2+}$, and two adjacent cations form π–π stacking in the $HL^{H,Me}$ ligands between the two quinolyl rings, which produce a 2D extended structure. Furthermore, the intralayer spaces of the 2D network are tightly occupied with only $CF_3SO_3^-$ ions, while those of the corresponding ClO_4^- compound are occupied with ClO_4^- ions and MeCN molecules. Hydrogen bond lengths and intermolecular C···C contacts are O(1)···N(1) = 2.883(4), O(1)···N(1)** = 3.061(3), N(1)**···O(1)** = 2.883(4), N(1)···O(1)** =

Table 2. Relevant Coordination Bond Lengths (Å), Angles (degree) for $[Fe^{II}(HL^{H,Me})_2](CF_3SO_3)_2$ at 296 and 100 K[a]

	296 K	100 K
Bond lengths		
Fe–N(2)	2.174(3)	1.9654(19)
Fe–N(3)	2.1220(19)	1.9337(17)
Fe–N(4)	2.183(2)	2.0363(18)
Fe–N(2)*	2.174(3)	1.9654(19)
Fe–N(3)*	2.1220(19)	1.9337(17)
Fe–N(4)*	2.183(2)	2.0363(18)
Bond angles		
N(2)–Fe–N(2)*	89.64(9)	90.09(8)
N(2)–Fe–N(3)	76.00(8)	80.54(7)
N(2)–Fe–N(3)*	90.78(8)	89.73(7)
N(2)–Fe–N(4)	152.01(7)	162.31(6)
N(2)–Fe–N(4)*	93.13(9)	91.27(8)
N(2)*–Fe–N(3)	90.78(8)	89.73(7)
N(2)*–Fe–N(3)*	76.00(8)	80.54(7)
N(2)*–Fe–N(4)	93.13(9)	91.27(8)
N(2)*–Fe–N(4)*	152.01(7)	162.31(6)
N(3)–Fe–N(3)*	161.48(8)	166.25(8)
N(3)–Fe–N(4)	76.12(8)	81.84(7)
N(3)–Fe–N(4)*	116.91(9)	107.89(8)
N(3)*–Fe–N(4)	116.91(9)	107.89(8)
N(3)*–Fe–N(4)*	76.12(8)	81.84(7)
N(4)–Fe–N(4)*	97.26(8)	92.75(8)

a) Symmetry operations: (*), $-x + 1, y, -z + 3/2$.

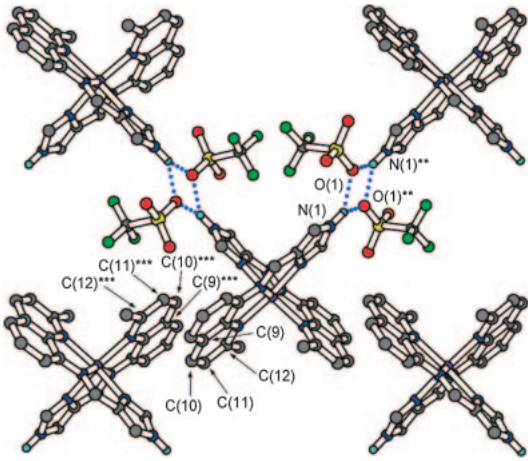

Figure 3. Intermolecular interactions of $[Fe^{II}(HL^{H,Me})_2](CF_3SO_3)_2$ at 296 K. Two $CF_3SO_3^-$ ions are bifurcate hydrogen-bonded to the imidazole NH groups of two neighboring cations $[Fe^{II}(HL^{H,Me})_2]^{2+}$, and two adjacent cations form π–π stacking in the $HL^{H,Me}$ ligands between the two quinolyl rings. The symbols, ** and ***, denote the symmetry operations of $-x+1$, $-y+1$, $-z+2$ and $-x+1$, $-y$, $-z+1$, respectively.

Table 3. Hydrogen Bond Lengths (Å) and Intermolecular C···C Contacts (Å) Shorter than the van der Waals Distance (3.6 Å) for $[Fe^{II}(HL^{H,Me})_2](CF_3SO_3)_2$ at 296 and 100 K[a)]

	296 K	100 K
Hydrogen bonds		
O(1)···N(1)	2.883(4)	2.903(3)
O(1)···N(1)**	3.061(3)	2.834(3)
N(1)**···O(1)**	2.883(4)	2.903(3)
N(1)···O(1)**	3.061(3)	2.834(3)
Intermolecular C···C contacts		
C(9)···C(11)***		3.409(4)
C(10)···C(11)***	3.562(5)	3.432(4)
C(10)···C(12)***	3.402(5)	3.371(4)
C(11)···C(9)***		3.409(4)
C(11)···C(10)***	3.562(5)	3.432(4)
C(11)···C(11)***	3.567(5)	
C(12)···C(10)***	3.402(5)	3.371(4)

a) Symmetry operations: (**), $-x+1$, $-y+1$, $-z+2$; (***), $-x+1$, $-y$, $-z+1$.

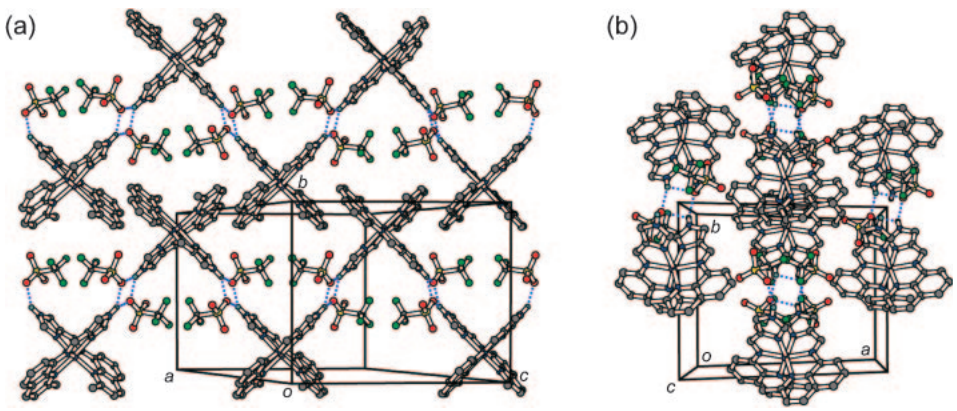

Figure 4. (a) Top view of a 2D extended structure of $[Fe^{II}(HL^{H,Me})_2](CF_3SO_3)_2$ at 296 K. The 2D layer is formed by bifurcated hydrogen bonds and π–π interactions and is parallel to the *bc* plane. The intralayer spaces of the 2D network are tightly occupied with only $CF_3SO_3^-$ ions. (b) Side view showing the stacking of the 2D extended structures. Each 2D layer assumes a thickness corresponding to one complex-molecular size and accumulates in the *a* direction.

3.061(3), C(10)···C(11)*** = 3.562(5), C(10)···C(12)*** = 3.402(5), C(11)···C(10)*** = 3.562(5), C(11)···C(11)*** = 3.567(5), and C(12)···C(10)*** = 3.402(5) Å at 296 K, as shown in Table 3. It should be noted that all imidazole NH groups and quinolyl rings of the $[Fe^{II}(HL^{H,Me})_2]^{2+}$ cation participate in the construction of the 2D extended structure. As shown in Figure 4b, each 2D layer assumes a thickness corresponding to one complex-molecular size, and the 2D layer is parallel to the *bc* plane and accumulates in the *a* direction. In the *a* direction, the 2D layers are connected mainly from weaker van der Waals interactions.

At 100 K: The complex assumes an octahedral coordination environment similar to that of 296 K. At 100 K, the Fe–N bond lengths (1.9337(17)–2.0363(18) Å) are typical for the LS Fe^{II} complex. The average Fe–N bond length decreases by 0.182 Å from 2.160 Å at 296 K to 1.978 Å at 100 K, and the difference of 0.182 Å is in a range typical for N_6 coordinated iron(II) SCO complexes.[1c] The N–Fe–N bond angles also indicate the spin state of the Fe^{II} ion, since the angles at 100 K are closer to a regular octahedron than that at 296 K (for example, N(2)–Fe–N(3), 76.00(8)° at 296 K, 80.54(7)° at 100 K).

The extended network structure is similar to that of 296 K. The slight difference is the lengths of intermolecular interactions. Hydrogen bond lengths and intermolecular C···C contacts are O(1)···N(1) = 2.903(3), O(1)···N(1)** = 2.834(3), N(1)**···O(1)** = 2.903(3), N(1)···O(1)** = 2.834(3), C(9)···C(11)*** = 3.409(4), C(10)···C(11)*** = 3.432(4), C(10)···C(12)*** = 3.371(4), C(11)···C(9)*** = 3.409(4), C(11)···C(10)*** = 3.432(4), and C(12)···C(10)*** = 3.371(4) Å at 100 K (Table 3). Hydrogen bond lengths are shorter than those at 296 K, and there are more

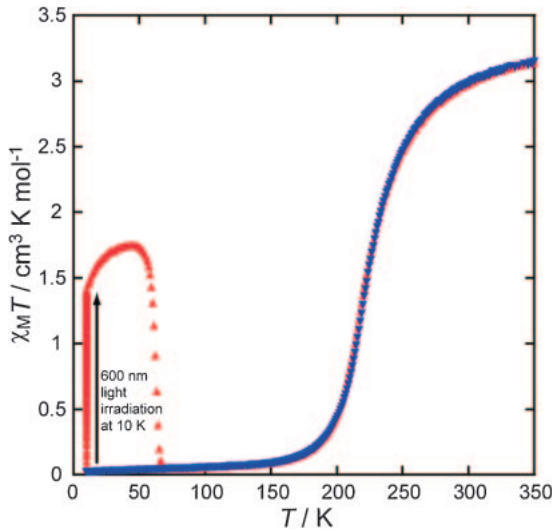

Figure 5. LIESST effect of $[Fe^{II}(HL^{H,Me})_2](CF_3SO_3)_2$. Light irradiation with wavelength of 600 nm at 10 K afforded an increase of the $\chi_M T$ value. After the light irradiation (600 nm) was switched off, the thermal relaxation process was recorded from 5 to 350 K in the warming mode (▲) and then the $\chi_M T$ value from 350 to 5 K in the cooling mode (▼) was measured.

intermolecular C···C contacts, which are shorter than those at 296 K. It should be noted that the spin transition of the $CF_3SO_3^-$ salt is more gradual than that of desolvated ClO_4^- salt and the hysteresis is absent, which is observed in ClO_4^- salt, although the intermolecular C···C contact of the $CF_3SO_3^-$ salt is shorter than that of ClO_4^- salt.[11]

LIESST Effect of $[Fe^{II}(HL^{H,Me})_2](CF_3SO_3)_2$. A LIESST experiment was performed.[12] The sample was placed at the edge of an optical fiber, where the power of the light was 2 mW cm^{-2}. Light irradiation at 600 nm of the polycrystalline sample passed through an interference filter with an 80 nm FWHM at 10 K afford an increase of the $\chi_M T$ value to reach the saturated value. The increase in the $\chi_M T$ value at 10 K during the light irradiation is attributed to the spin transition from the LS to HS state. As shown in Figure 5, the saturated $\chi_M T$ value of ca. 1.4 cm^3 K mol^{-1} at 10 K is smaller than the expected value of HS Fe^{II}. After the light was switched off, the thermal relaxation was studied. Upon elevating the temperature, the $\chi_M T$ value increases and reaches the maximum value of ca. 1.7 cm^3 K mol^{-1} at 44 K and then abruptly decreases around 60 K. The maximum value of ca. 1.7 cm^3 K mol^{-1} at 44 K suggests that about half of the Fe^{II} sites convert from the LS to HS state due to LIESST. The limit LIESST temperature, T(LIESST),[13] which was evaluated from the first derivative of $\chi_M T$ in the HS → LS relaxation after LIESST, is 63 K, where it should be noted that the value is evaluated from the data with 1 K min^{-1} sweeping mode.

Effect of the Crystal Packing on the SCO of $[Fe^{II}(HL^{H,Me})_2](CF_3SO_3)_2$ and $[Fe^{II}(HL^{H,Me})_2](ClO_4)_2$·1.5MeCN. In this work, we synthesized a 2D SCO iron(II) complex, $[Fe^{II}(HL^{H,Me})_2](CF_3SO_3)_2$, in hope to investigate in more detail the effect of the crystal packing on the SCO properties in comparison with the data of the corresponding ClO_4^- complex, $[Fe^{II}(HL^{H,Me})_2](ClO_4)_2$·1.5MeCN.[11] Since the present $CF_3SO_3^-$ salt is isomorphous to the corresponding ClO_4^- salt, the correlation between the crystal packing and the SCO parameters of the $CF_3SO_3^-$ salt can be compared to those of the ClO_4^- salt.

Table 4. Selected Parameters of $[Fe^{II}(HL^{H,Me})_2](CF_3SO_3)_2$ and Desolvated ClO_4^- Salt, $[Fe^{II}(HL^{H,Me})_2](ClO_4)_2$[11] for Comparing Their SCO Properties

SCO parameters	Complex	
	$[Fe^{II}(HL^{H,Me})_2]$-$(CF_3SO_3)_2$	$[Fe^{II}(HL^{H,Me})_2]$-$(ClO_4)_2$[11]
Transition pattern	gradual	steep
$T_{1/2\uparrow}$/K	215	185
$T_{1/2\downarrow}$/K	215	174
$T_{1/2\ (average)}$/K	215	180
Hysteresis/K	0	11

Table 4 shows the parameters of the SCO transition of the $CF_3SO_3^-$ salt and the ClO_4^- salt. The $CF_3SO_3^-$ salt has no crystal solvent, and shows a gradual and reversible one-step spin transition between the HS ($S = 2$) and LS ($S = 0$) states at $T_{1/2} = 215$ K without hysteresis, while the ClO_4^- salt has MeCN as the crystal solvent, and shows a desolvation induced steep one-step spin transition at $T_{1/2\uparrow} = 185$ K and $T_{1/2\downarrow} = 174$ K with a hysteresis of 11 K. The $T_{1/2}$ value of the $CF_3SO_3^-$ salt is higher than that of corresponding desolvated ClO_4^- salt, about 35 K, although the spin transition is more gradual than that of ClO_4^- salt and the hysteresis is absent, which is observed in ClO_4^- salt.

The most different feature between two complexes is the packing of the intralayer spaces of the 2D network. Although the volume of the two complexes at 296 K is almost the same and only the ClO_4^- salt has one MeCN molecule as the crystal solvent occupying the intralayer cavity of the 2D network, the density of the $CF_3SO_3^-$ salt is higher than that of the ClO_4^- salt. It can be explained by the shape and volume of the counter anions evaluated by quantum-chemical calculations (86.9 Å^3 for $CF_3SO_3^-$ and 54.4 Å^3 for ClO_4^-).[14] Since the $CF_3SO_3^-$ ion has a dumbbell-like shape and is larger than the sphere-like ClO_4^- ion, the intralayer spaces of the 2D network are occupied by only the counter anions and there are no crystal solvents in $CF_3SO_3^-$ salt. As a result, the crystal packing of $CF_3SO_3^-$ salt is tighter than that of ClO_4^- salt and large structural change is limited. Additionally, the $CF_3SO_3^-$ salt has no other molecules between the 2D layers which can interact with the SCO sites of each layer, while the ClO_4^- salt has 0.5MeCN molecules in the interlayer cavity between the 2D layers, which may affect the interlayer interaction between the SCO sites by desolvation of it. It suggests that SCO is very sensitive to the tightness and flexibility of network structure which is strongly affected by the crystal packing correlated with the space-occupying molecules.

Conclusion

In summary, a 2D SCO iron(II) complex, $[Fe^{II}(HL^{H,Me})_2]$-$(CF_3SO_3)_2$, was synthesized, where $HL^{H,Me}$: tridentate N_3 Schiff-base ligand of the 1:1 condensation product of 4-formyl-

imidazole and 8-amino-2-methylquinoline, and its structures and magnetic properties were investigated. Since the present 2D $CF_3SO_3^-$ complex, $[Fe^{II}(HL^{H,Me})_2](CF_3SO_3)_2$, was isomorphous to the corresponding ClO_4^- salt, $[Fe^{II}(HL^{H,Me})_2](ClO_4)_2 \cdot 1.5MeCN$, the correlation between the crystal packing and the SCO parameters of the $CF_3SO_3^-$ salt was compared to those of the ClO_4^- salt. Comparison of the results of $CF_3SO_3^-$ salt, $[Fe^{II}(HL^{H,Me})_2](CF_3SO_3)_2$, and the data of the corresponding ClO_4^- salt, $[Fe^{II}(HL^{H,Me})_2](ClO_4)_2 \cdot 1.5MeCN$, demonstrates that the slight difference of their crystal packing due to the space-occupying molecules causes the drastic change of the SCO properties, such as transition temperature, gradual or steep transition, and with or without hysteresis. In addition, LIESST was observed in the $CF_3SO_3^-$ salt. In this compound, 600 nm light irradiation at 10 K showed that about half of the Fe^{II} sites converted from the LS to HS state. The present result can add to better understanding of SCO phenomenon.

Experimental

Materials. All chemicals and solvents, obtained from Tokyo Kasei Co., Ltd., and Wako Pure Chemical Industries, Ltd., were of reagent grade and used for syntheses without further purification.

Preparation. $[Fe^{II}(HL^{H,Me})_2](CF_3SO_3)_2$: All the synthetic procedures were carried out in air. A solution of 8-amino-2-methylquinoline (0.316 g, 2 mmol) in 5 mL of methanol was added to a solution of 4-formylimidazole (0.192 g, 2 mmol) in 5 mL of methanol. The mixture was stirred on a hot plate at 40 °C for 2 h. The methanolic solution of the tridentate ligand thus prepared was used without isolation of the ligand for the synthesis of the metal complex. A solution of $Fe^{II}(CF_3SO_3)_2$ (0.354 g, 1 mmol) in 5 mL of methanol was added to the ligand solution (2 mmol). The resulting solution was stirred for 15 min and then filtered. The filtrate was allowed to stand for several days, during which time the precipitated black block crystals were collected by suction filtration. Yield: 0.620 g (75%). Anal. Calcd for $[Fe^{II}(HL^{H,Me})_2](CF_3SO_3)_2 = C_{30}H_{24}N_8F_6S_2O_6Fe$: C, 43.59; H, 2.93; N, 13.56%. Found: C, 43.79; H, 3.18; N, 13.48%. IR (KBr): $\nu_{C=N}$ 1610 cm^{-1}, $\nu_{CF_3SO_3}$ 1274 cm^{-1}.

Physical Measurements. Elemental C, H, and N analyses were carried out by Miss Kikue Nishiyama at the Center for Instrumental Analysis of Kumamoto University. Infrared spectra were recorded at room temperature using a Nicolet Avatar 370 DTGS (Thermo Electron Corporation) spectrometer with samples in KBr disks. Magnetic susceptibilities were measured in the 5–350 K temperature range, at a sweep rate of 1 K min^{-1}, under an applied magnetic field of 0.5 T, using a MPMS5 SQUID susceptometer (Quantum Design). The apparatus was calibrated with palladium metal. Corrections for diamagnetism were applied by using Pascal's constants.[15] For the LIESST experiment, a xenon arc lamp (Hamamatsu L7810) was used as the light source. The light passes through an interference filter and was guided via an optical fiber into the SQUID magnetometer. The sample was placed on the edge of an optical fiber. The measurements were performed on a very thin layer of powder sample. The weight was estimated by comparing the thermal spin crossover curve with that for a heavier and accurately weighed sample.

X-ray Crystallography. A black block crystal having approximate dimensions of $0.25 \times 0.27 \times 0.33\,mm^3$ was mounted on a glass fiber. All measurements were made on a Rigaku RAXIS RAPID imaging plate area detector with graphite monochromated Mo Kα radiation ($\lambda = 0.71075$ Å), using the same crystal. The temperature of the crystal was maintained at the selected value by means of a Rigaku cooling device to within an accuracy of ± 2 K. The data were corrected for Lorentz, polarization, and absorption effects. The structures were solved by direct methods and expanded using Fourier technique. The structures were refined on F^2 full-matrix least-squares with anisotropic displacement parameters for all non-hydrogen atoms. Hydrogen atoms were fixed at the calculated positions and refined using a riding model. All calculations were performed using the Crystal Structure crystallographic software package.[16,17]

X-ray Crystallographic data in CIF format for $[Fe^{II}(HL^{H,Me})_2](CF_3SO_3)_2$ at 296 and 100 K have been deposited with the deposition numbers 824853 and 824854 at CCDC. Copies of the data can be obtained free of charge via http://www.ccdc.cam.ac.uk/conts/retrieving.html (or from the Cambridge Crystallographic Data Centre, 12, Union Road, Cambridge, CB2 1EZ, U.K.; Fax: +44 1223 336033; e-mail: deposit@ccdc.cam.ac.uk).

References

1 a) *Spin Crossover in Transition Metal Compounds I* in *Topics in Current Chemistry*, ed. by P. Gütlich, H. A. Goodwin, Springer, Berlin, **2004**, Vol. 233. doi:10.1007/b40394-9; *Spin Crossover in Transition Metal Compounds II* in *Topics in Current Chemistry*, ed. by P. Gütlich, H. A. Goodwin, Springer, Berlin, **2004**, Vol. 234. doi:10.1007/b93641; *Spin Crossover in Transition Metal Compounds III* in *Topics in Current Chemistry*, ed. by P. Gütlich, H. A. Goodwin, Springer, Berlin, **2004**, Vol. 235. doi:10.1007/b96439. b) P. Gütlich, Y. Garcia, H. A. Goodwin, *Chem. Soc. Rev.* **2000**, *29*, 419. c) P. Gütlich, A. Hauser, H. Spiering, *Angew. Chem., Int. Ed. Engl.* **1994**, *33*, 2024. d) H. A. Goodwin, *Coord. Chem. Rev.* **1976**, *18*, 293. e) P. Gütlich, *Struct. Bonding* **1981**, *44*, 83. f) E. König, G. Ritter, S. K. Kulshreshtha, *Chem. Rev.* **1985**, *85*, 219. g) E. König, *Struct. Bonding* **1991**, *76*, 51. h) J. A. Real, A. B. Gaspar, V. Niel, M. C. Muñoz, *Coord. Chem. Rev.* **2003**, *236*, 121.

2 a) O. Kahn, C. J. Martinez, *Science* **1998**, *279*, 44. b) J. A. Real, E. Andres, M. C. Muñoz, M. Julve, T. Granier, A. Bousseksou, F. Varret, *Science* **1995**, *268*, 265. c) P. J. van Koningsbruggen, Y. Garcia, O. Kahn, L. Fournès, H. Kooijman, A. L. Spek, J. G. Haasnoot, J. Moscovici, K. Provost, A. Michalowicz, F. Renz, P. Gütlich, *Inorg. Chem.* **2000**, *39*, 1891. d) S. Hayami, K. Danjobara, K. Inoue, Y. Ogawa, N. Matsumoto, Y. Maeda, *Adv. Mater.* **2004**, *16*, 869. e) O. Kahn, J. P. Launay, *Chemtronics* **1988**, *3*, 140.

3 a) G. J. Halder, C. J. Kepert, B. Moubaraki, K. S. Murray, J. D. Cashion, *Science* **2002**, *298*, 1762. b) J. Kröber, E. Codjovi, O. Kahn, F. Groliere, C. Jay, *J. Am. Chem. Soc.* **1993**, *115*, 9810. c) A. Galet, M. C. Muñoz, A. B. Gaspar, J. A. Real, *Inorg. Chem.* **2005**, *44*, 8749. d) P. J. van Koningsbruggen, Y. Garcia, E. Codjovi, R. Lapouyade, O. Kahn, L. Fournès, L. Rabardel, *J. Mater. Chem.* **1997**, *7*, 2069. e) S. Imatomi, T. Sato, S. Hashimoto, N. Matsumoto, *Eur. J. Inorg. Chem.* **2009**, 721.

4 a) T. Buchen, P. Gütlich, K. H. Sugiyarto, H. A. Goodwin,

Chem.—Eur. J. **1996**, *2*, 1134. b) K. H. Sugiyarto, M. L. Scudder, D. C. Craig, H. A. Goodwin, *Aust. J. Chem.* **2000**, *53*, 755. c) K. H. Sugiyarto, H. A. Goodwin, *Aust. J. Chem.* **1988**, *41*, 1645. d) T. Sato, S. Iijima, M. Kojima, N. Matsumoto, *Chem. Lett.* **2009**, *38*, 178. e) S. Arata, T. Hamamatsu, T. Sato, T. Iihoshi, N. Matsumoto, S. Iijima, *Chem. Lett.* **2007**, *36*, 778. f) H. Torigoe, H. Hagiwara, S. Arata, M. Yamada, N. Matsumoto, *Chem. Lett.* **2005**, *34*, 956.

5 S. Hayami, Z. Gu, M. Shiro, Y. Einaga, A. Fujishima, O. Sato, *J. Am. Chem. Soc.* **2000**, *122*, 7126.

6 a) J. Wajnflasz, R. Pick, *J. Phys., Colloq.* **1971**, *32*, C1-91. b) A. Bousseksou, F. Varret, J. Nasser, *J. Phys. I* **1993**, *3*, 1463. c) M. Nishino, K. Boukheddaden, S. Miyashita, F. Varret, *Phys. Rev. B* **2003**, *68*, 224402.

7 a) M. Nishino, K. Boukheddaden, Y. Konishi, S. Miyashita, *Phys. Rev. Lett.* **2007**, *98*, 247203. b) Y. Konishi, H. Tokoro, M. Nishino, S. Miyashita, *Phys. Rev. Lett.* **2008**, *100*, 067206. c) S. Miyashita, Y. Konishi, M. Nishino, H. Tokoro, P. A. Rikvold, *Phys. Rev. B* **2008**, *77*, 014105. d) N. Willenbacher, H. Spiering, *J. Phys. C: Solid State Phys.* **1988**, *21*, 1423. e) H. Spiering, N. Willenbacher, *J. Phys.: Condens. Matter* **1989**, *1*, 10089. f) M. M. Dîrtu, C. Neuhausen, A. D. Naik, A. Rotaru, L. Spinu, Y. Garcia, *Inorg. Chem.* **2010**, *49*, 5723.

8 a) Y. Sunatsuki, Y. Ikuta, N. Matsumoto, H. Ohta, M. Kojima, S. Iijima, S. Hayami, Y. Maeda, S. Kaizaki, F. Dahan, J.-P. Tuchagues, *Angew. Chem., Int. Ed.* **2003**, *42*, 1614. b) Y. Ikuta, M. Ooidemizu, Y. Yamahata, M. Yamada, S. Osa, N. Matsumoto, S. Iijima, Y. Sunatsuki, M. Kojima, F. Dahan, J.-P. Tuchagues, *Inorg. Chem.* **2003**, *42*, 7001.

9 a) M. Yamada, H. Hagiwara, H. Torigoe, N. Matsumoto, M. Kojima, F. Dahan, J.-P. Tuchagues, N. Re, S. Iijima, *Chem.—Eur. J.* **2006**, *12*, 4536. b) H. Hagiwara, N. Matsumoto, S. Iijima, M. Kojima, *Inorg. Chim. Acta* **2011**, *366*, 283.

10 a) C. Brewer, G. Brewer, G. Patil, Y. Sun, C. Viragh, R. J. Butcher, *Inorg. Chim. Acta* **2005**, *358*, 3441. b) G. Brewer, M. J. Olida, A. M. Schmiedekamp, C. Viragh, P. Y. Zavalij, *Dalton Trans.* **2006**, 5617. c) C. Brewer, G. Brewer, R. J. Butcher, E. E. Carpenter, L. Cuenca, B. C. Noll, W. R. Scheidt, C. Viragh, P. Y. Zavalij, D. Zielaski, *Dalton Trans.* **2006**, 1009.

11 H. Hagiwara, S. Hashimoto, N. Matsumoto, S. Iijima, *Inorg. Chem.* **2007**, *46*, 3136.

12 a) S. Decurtins, P. Gütlich, C. P. Köhler, H. Spiering, A. Hauser, *Chem. Phys. Lett.* **1984**, *105*, 1. b) A. Hauser, *Spin Crossover in Transition Metal Compounds II* in *Topics in Current Chemistry*, ed. by P. Gütlich, H. A. Goodwin, Springer, Berlin, **2004**, Vol. 234, pp. 155–198. doi:10.1007/b95416.

13 J.-F. Létard, P. Guionneau, O. Nguyen, J. S. Costa, S. Marcén, G. Chastanet, M. Marchivie, L. Goux-Capes, *Chem.—Eur. J.* **2005**, *11*, 4582.

14 *Spartan, Version 4.0*, Wavefunction, Inc., Irvine, California, **1999**.

15 O. Kahn, *Molecular Magnetism*, VCH, Weinheim, **1993**.

16 *CrystalStructure 4.0: Crystal Structure Analysis Package*, Rigaku Corporation, Tokyo, Japan, **2000–2010**.

17 J. R. Carruthers, J. S. Rollett, P. W. Betteridge, D. Kinna, L. Pearce, A. Larsen, E. Gabe, *CRYSTALS Issue 11*, Chemical Crystallography Laboratory, Oxford, UK, **1999**.